Multiple Cell Tracking Using Ant Estimator

Benlian Xu, Mingli Lu, Peiyi Zhu, Qinglan Chen, and Xiaoying Wang

Abstract—Quantitative analysis of cell dynamic processes through fluorescence microscopy imaging requires simultaneously tracking large and time-varying number of bright spots and its individual states in noisy image sequences. Such process is characterized as a challenging task due to several roadblocks including the severe image noise and clutter, the occlusion of one cell by others, and the weak image contrast. In this paper, we propose a novel ant stochastic searching behavior based tracking algorithm, which is called ANT estimator, to tracking multiple cells in fluorescence image sequences. In our ant system, each ant determines probabilistically potential state and then adjusts its mobility according to cell detection position heuristic information. Simulation results verify the effectiveness of our algorithm when applied to cell tracking cases, and its performance is also compared with the particle filter based cell tracking algorithm.

I. INTRODUCTION

THE ability to visualize cells dynamic processes in space and time has been made possible by revolutionary developments in imaging technology in the past two decades. In terms of hardware, advances in optical systems design have taken light microscopy from widefield to confocal and spinning disk microscopy [1-3], and this in turn results in vast amount of dynamic image data. With large time span and more cells being concerned, data exploration is inevitable, and general methods of processing image data do not guarantee sufficient speed, accuracy, and reproducibility. Therefore, many efforts have been made to develop novel and effective cell tracking techniques.

Generally speaking, previous work on cell tracking can be classified into deterministic tracking and stochastic tracking [4]. Deterministic tracking usually relies on accurate and reliable segmentation results, and sometimes yields poor performance for severe image quality. Meanwhile, stochastic tracking is usually characterized as a parameter estimation problem, in which a stochastic state transition model and observation model between the target state and the image intensity observation are first built, and then appropriate multi-target algorithms [5-8] are required to approximate the evolution of the target state. It is recognized that the stochastic tracking is a preferred automated tracking method, since it can replace tedious manual procedures and eliminate the bias and variability in human judgments. Particle Filter (PF) is a widely used non-linear non-Gaussian parameter filtering algorithm, and the use of PF in combination with level-sets [9] and active contours [10] has been reported and achieved better performance than deterministic methods for biological cell [11].

Ant Colony Optimization (ACO) makes use of simple agents called ants which iteratively build candidate solutions to a combinatorial optimization problem, and the ants' solution construction is guided by pheromone trails and problem-dependent heuristic information. It is observed that generic ACO algorithm could be successfully applied to any combinatorial optimization problem [12], and its variants to parameter estimation field as well [13,14]. Inspired by ant stochastic searching behavior, we develop a suitable ANT Estimator, a colony of moving ants each represented by individual state, for tracking simultaneously large number of cells in 2-D dynamic fluorescence microscopy images.

The paper is organized as follows. In Section II, we first describe the background of PF, and then give the idea origin of ant estimator . In Section III, the ant estimator for multiple cells is designed and analysized as well. Simulation results are given for demonstrating the superior performance of our algorithm in Section IV.

II. BACKGROUND

A. Particle Filter and It's Application to Cell Tracking

In general, the state of each cell evolves in a non-linear way, and this case is just suitable for the application of particle filter. We assume that the dynamic model of each cell is described as

$$\begin{aligned} \boldsymbol{x}_{t+1} &= f(\boldsymbol{x}_t, \boldsymbol{w}_t) \\ \boldsymbol{z}_t &= h(\boldsymbol{x}_t, \boldsymbol{v}_t) \end{aligned} \tag{1}$$

where $\boldsymbol{x}_t \in R^{n_x}$ denotes the state at time t, $\boldsymbol{z}_t \in R^{n_z}$ is the corresponding measurement, $\boldsymbol{w}_t$ and $\boldsymbol{v}_t$ represent the process and measurement noise, respectively. In the above formula, the system model is assumed to follow the first order Markov density function $p_{t|t-1}(\boldsymbol{x}_t \mid \boldsymbol{x}_{t-1})$ on the state space $\chi \subseteq \Re^{Rn_x}$, and the observation function $h(\cdot)$ is usually modeled as a likelihood function $p_t(\boldsymbol{z}_t \mid \boldsymbol{x}_t)$ on the observation space $Z \subseteq R^{n_z}$, respectively.

Given an initial density function $\pi_0(\boldsymbol{x}_0)$ of state, the posterior filtering density at time t can be calculated by the Bayesian recursion

$$\pi_{t|t-1}(\boldsymbol{x}_t \mid \boldsymbol{z}_{1:t-1}) = \int p_{t|t-1}(\boldsymbol{x}_t \mid \boldsymbol{x}) \pi_{t-1|t-1}(\boldsymbol{x} \mid \boldsymbol{z}_{1:t-1}) d\boldsymbol{x} \tag{2}$$

$$\pi_{t|t}(\boldsymbol{x}_t \mid \boldsymbol{z}_{1:t}) = \frac{p_t(\boldsymbol{z}_t \mid \boldsymbol{x}_t) \pi_{t|t-1}(\boldsymbol{x}_t \mid \boldsymbol{z}_{1:t-1})}{\int p_t(\boldsymbol{z}_t \mid \boldsymbol{x}) \pi_{t|t-1}(\boldsymbol{x} \mid \boldsymbol{z}_{1:t-1}) d\boldsymbol{x}} \tag{3}$$

Benlian Xu is with the Changshu Institute of Technology, Changshu, P. R. China, 215500 (e-mail:xu_benlian@ yahoo.com.cn).

where $z_{1:t} = \{z_1, z_2, ..., z_t\}$ denotes the accumulated observations up to time t. Once the posterior probabilistic density function $\pi_{t|t}(\boldsymbol{x}_t \mid \boldsymbol{z}_{1:t})$ is available, the corresponding estimate of state $\boldsymbol{x}_t$ can be achieved by the maximum a posterior (MAP) estimator.

To implement the Bayesian recursion, a direct and easy alternative is the PF or Sequential Monte-Carlo technique.

Initialization: Drawing N samples equally $\{x_0^{(i)}, N^{-1}\}_{i=1}^{N}$ from the initial cell state density function $\pi_{0|0}$, thus we have

$$\pi_{t-1}(\boldsymbol{x}_{t-1} \mid \boldsymbol{z}_{1:t-1}) = \frac{1}{N}\sum_{i=1}^{N}\delta_{\boldsymbol{x}_{t-1}^{(i)}}(\boldsymbol{x}_{t-1}) \tag{4}$$

where $\delta_{\boldsymbol{x}_{t-1}^{(i)}}(\cdot)$ denotes the delta-Dirac function centered at $x_{t-1}^{(i)}$.

Prediction step: This step is done for each particle to obtain predicted particle $\bar{x}_t^{(i)}$ using the proposal density function

$$\bar{\boldsymbol{x}}_t^{(i)} = q_t(\cdot \mid \boldsymbol{x}_{t-1}^{(i)}, \boldsymbol{z}_t) \quad i = 1, 2, ..., N \tag{5}$$

And the predicted weight for each particle is

$$w_{t|t-1}^{(i)} = \frac{p_{t|t-1}(\bar{\boldsymbol{x}}_t^{(i)} \mid \boldsymbol{x}_{t-1}^{(i)})}{q_t(\bar{\boldsymbol{x}}_t^{(i)} \mid \boldsymbol{x}_{t-1}^{(i)}, \boldsymbol{z}_t)} w_{t-1}^{(i)} \tag{6}$$

Thus, the one-step predicted distribution is obtained

$$\pi_{t|t-1}(\boldsymbol{x}_t \mid \boldsymbol{z}_{1:t-1}) = \sum_{i=1}^{N} w_{t|t-1}^{(i)} \delta_{\bar{\boldsymbol{x}}_t^{(i)}}(\boldsymbol{x}_t) \tag{7}$$

Update step: Once new detected cell image measurement $\boldsymbol{z}_t$ at time t is available, and if Eq. (7) is substituted into Eq. (3), we have the Monte-Carlo approximation

$$\pi_{t|t}(\boldsymbol{x}_t \mid \boldsymbol{z}_{1:t}) = \sum_{i=1}^{N}\left(\frac{w_{t|t-1}^{(i)} p_t(\boldsymbol{z}_t \mid \bar{\boldsymbol{x}}_t^{(i)})}{\sum_{i=1}^{N} w_{t|t-1}^{(i)} p_t(\boldsymbol{z}_t \mid \bar{\boldsymbol{x}}_t^{(i)})}\right)\delta_{\bar{\boldsymbol{x}}_t^{(i)}}(\boldsymbol{x}_t) \tag{8}$$

The last term in Eq. (8) can be further reduced to a simplified form in terms of updated weight, thus Eq. (8) becomes

$$\pi_{t|t}(\boldsymbol{x}_t \mid \boldsymbol{z}_{1:t}) = \sum_{i=1}^{N} w_t^{(i)} \delta_{\bar{\boldsymbol{x}}_t^{(i)}}(\boldsymbol{x}_t) \tag{9}$$

where $w_t^{(i)} = \dfrac{p_t(\boldsymbol{z}_t \mid \bar{\boldsymbol{x}}_t^{(i)})}{\sum_{i=1}^{N} w_{t|t-1}^{(i)} p_t(\boldsymbol{z}_t \mid \bar{\boldsymbol{x}}_t^{(i)})} w_{t|t-1}^{(i)}$.

Re-sampling step: Finally, the re-sampling step is performed to obtain a set of un-weighted particles $\{x_t^{(i)}, N^{-1}\}_{i=1}^{N}$ for the following iteration, and these particles constitute the approximate distribution of state

$$\pi_{t|t}(\boldsymbol{x}_t \mid \boldsymbol{z}_{1:t}) = \frac{1}{N}\sum_{i=1}^{N}\delta_{\boldsymbol{x}_t^{(i)}}(\boldsymbol{x}_t) \tag{10}$$

Finally, the estimate for $\boldsymbol{x}_t$ at time t is the mean sum of each state $\{x_t^{(i)}, N^{-1}\}_{i=1}^{N}$.

B. Inspiration From Ant Stochastic Search

In real world ant system, each ant starts from their nest and find food source through collaboration. During the initial phase, all ants are distributed randomly in the searching field, as shown in Fig. 1(a), and keep on depositing chemical pheromone when moving from one place to another place. Once some ant finds the food source, it will move back and continue depositing large amount of pheromone on its back tour. For the following ants, this tour can be an indication to better one from nest to food, and prone to re-selecting and further modifications in later iterations. This process is modeled and known as ant colony optimization (ACO). Over the past two decades, many combination optimization problems have been solved successfully by ACO and its variants. It can be observed the food source is static rather than moving in traditional ant system, so we try to propose a novel ant system in which ant can search for moving food source. Using this concept, it is expected to design ANT Estimator, which is based on ant stochastic searching behavior, to track multiple cells, as shown in Fig. 1(b).

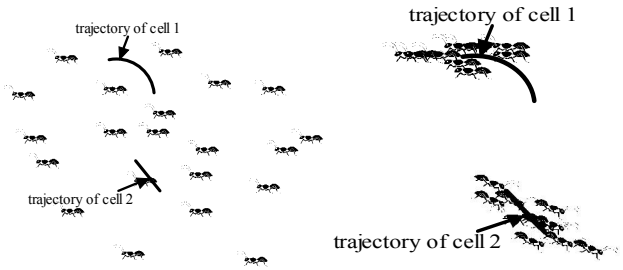

Fig. 1. Possibility of multi-cell tracking using ants' evolution

III. ANT ESTIMATOR FOR MULTIPLE CELL TRACKING

In this section we will specify the principle of our proposed ANT Estimator for cell tracking. Without loss of generality, the search model of some given ant k is modeled and investigated, and other ants could follow the process in the same manner.

Step1): To construct the next ant visiting space, the predicted state of each ant is required to calculate. For instance, assume that the state of ant k at time $t-1$ is known, the corresponding one step prediction state is obtained according to Eq. (1), which constitutes a potential state at time t to be visited by itself or other ants at time $t-1$.

Step2): For those predicted state above, we normalized the importance weights as below:

$$\tilde{w}^{(k)}(t) = w^{(k)}(t)\left[\sum_{j=1}^{N} w^{(j)}(t)\right]^{-1} \tag{11}$$

where $w^{(k)}(t) = p(\boldsymbol{y}(t) \mid \boldsymbol{x}^{(k)}(t \mid t-1)) = N(\boldsymbol{y}(t), \boldsymbol{x}^{(k)}(t \mid t-1), \boldsymbol{R}(t))$ with the assumption of Gaussian measurement noise.

Step3): Suppose that the movement of any given ant k from time $t-1$ to t could be decomposed into two decisions, as shown in Fig.2. Firstly, ant k at time $t-1$ moves directly toward its predicted state, i.e., from states $\boldsymbol{x}^{(k)}(t-1)$ to $\boldsymbol{x}^{(k)}(t \mid t-1)$. Afterwards, ant k will select the predicted state of ant j as its further moving direction based on the following defined probabilistic decision:

$$p_{k,j} = \frac{\tilde{w}^{(j)}(t)}{\sum_{j \neq k} \tilde{w}^{(j)}(t)} \tag{12}$$

But the moving distance of ant k needs to be determined and is utilized further to update the predicted state $\boldsymbol{x}^{(k)}(t \mid t-1)$. Consequently, the updated state of ant k is viewed as its estimated state at time t denoted by $\boldsymbol{x}^{(k)}(t)$.

According to the description above, ant k with state $\boldsymbol{x}^{(k)}(t-1)$ can move directly toward state $\boldsymbol{x}^{(k)}(t)$ in a sampling interval.

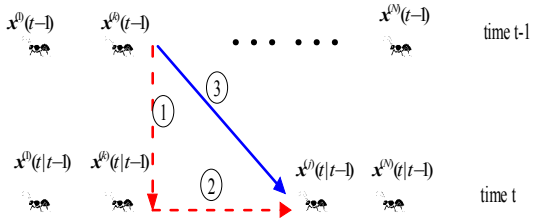

Fig.2 Movement behavior of ant from one time to another

Thus, if the state $x^{(j)}(t \mid t-1)$ is chosen as the destination direction of ant k starting from time $t-1$, and

$x^{(j)}(t \mid t-1) > x^{(k)}(t \mid t-1)$

$\tilde{w}^{(j)}(t) > \tilde{w}^{(k)}(t)$

we update the state of ant k at time t as follows

$$\dot{x}^{(k)}(t) = C_x(t) - G(t) * \Delta\dot{x}^{(k)}(t-1) \tag{13}$$

$$x^{(k)}(t) = x^{(k)}(t-1) + \dot{x}^{(k)}(t) * T \tag{14}$$

where T is the sampling interval; $C_x(t)$ denotes the predicted velocity in the x direction and given by $C_x(t) = \frac{\tilde{x}^{(j)}(t \mid t-1) - \tilde{x}^{(k)}(t-1)}{T}$. $\Delta\dot{x}^{(k)}(t-1)$ represents the moving ability of ant k in a given domain, which depends on its weight $\tilde{w}^{(k)}(t)$. $G(t)$ is an adjusting velocity coefficient and defined by $G(t) = \exp\left(-\frac{(\tilde{w}^{(j)} - \tilde{w}^{(k)})^2}{2\varepsilon^2}\right)$ with a constant ε. It can be observed that, if $\tilde{w}^{(j)}(t) >> \tilde{w}^{(k)}(t)$, it results in a smaller $G(t) * \Delta\dot{x}^{(k)}(t-1)$, thus the updated position of ant k will approach closer to the left side of $x^{(j)}(t \mid t-1)$, but if $\tilde{w}^{(j)}(t) \approx \tilde{w}^{(k)}(t)$, it is not the case due to large $G(t)$. For other cases, readers refer to Table 1.

Table.1 Moving rules for each ant

Condition	$x^{(j)}(t \mid t-1) > x^{(k)}(t \mid t-1)$	$x^{(j)}(t \mid t-1) < x^{(k)}(t \mid t-1)$
$\tilde{w}^{(j)}(t) > \tilde{w}^{(k)}(t)$	$\dot{x}^{(k)}(t) = C_x(t) - G(t) * \Delta\dot{x}^{(k)}(t-1)$	$\dot{x}^{(k)}(t) = C_x(t) + G(t) * \Delta\dot{x}^{(k)}(t-1)$
$\tilde{w}^{(j)}(t) \leq \tilde{w}^{(k)}(t)$	$\dot{x}^{(k)}(t) = \dot{x}^{(k)}(t-1) + q_1 * \Delta\dot{x}^{(k)}(t-1)$	$\dot{x}^{(k)}(t) = \dot{x}^{(k)}(t-1) - q_2 * \Delta\dot{x}^{(k)}(t-1)$

where q_1 and q_2 are random numbers.

When all ants at time $t-1$ have finished their selections, i.e., a set of updated states $\{x^{(k)}(t), k = 1, 2, \ldots N\}$ is obtained, the pheromone update process is executed. In this work, however, the updated pheromone refers to the moving ability of each ant $\Delta\dot{x}^{(\bullet)}(t)$. In order to perform the update process, two steps are required. Based on the current available measurement, the importance weights for all newly obtained states $\{x^{(k)}(t), k = 1, 2, \ldots N\}$ are now re-evaluated and normalized as below:

$$\tilde{w}'^{(k)}(t) = w'^{(k)}(t)\left[\sum_{j=1}^{N} w'^{(j)}(t)\right]^{-1} \tag{15}$$

where $w'^{(k)}(t) = p(\boldsymbol{y}(t) \mid \boldsymbol{x}^{(k)}(t)) = N(\boldsymbol{y}(t), \boldsymbol{x}^{(k)}(t), \boldsymbol{R}(t))$ with the assumption of Gaussian measurement noise.

Thus, the update moving ability of ant k, for instance, could be described as

$$\Delta\dot{x}^{(k)}(t) = \frac{\rho}{\tilde{w}'^{(k)}(t)} \Delta\dot{x}^{(k)}(t-1) \tag{16}$$

where ρ denotes the parameter balancing the importance of each ant. Here, we have $\rho = \frac{1}{N}\sum_{k=1}^{N} \tilde{w}'^{(k)}(t)$. Note that the update equation implies that, for an ant with larger weight, the corresponding moving ability decreases, i.e., those ants with larger weights may be located nearby the true state to be estimated, and be reluctant to move away from the current position. While for those ants with smaller weights, their moving abilities will increase, and enable them to make a "big step" towards the true state.

IV. Simulation Results And Discussion

The performance of our proposed ANT estimator is tested on real fluorescence microscopy image cell data with size of $50pix \times 50pix$, along with PF-based cell tracking algorithm. Altogether 50 ants in ANT Estimator and 50 particles in PF are used, the sampling interval $T = 10\,\text{min}$, and the initial state of each cell is given as $[z_x(0), z_y(0), 0, 0]$. It is noted that we take the detected measurements as cell initial state in x and y directions, respectively, and initial velocity is set to be zero.

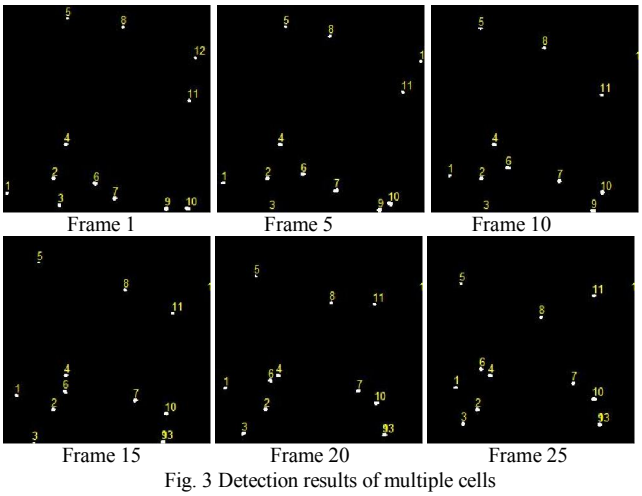

Fig. 3 Detection results of multiple cells

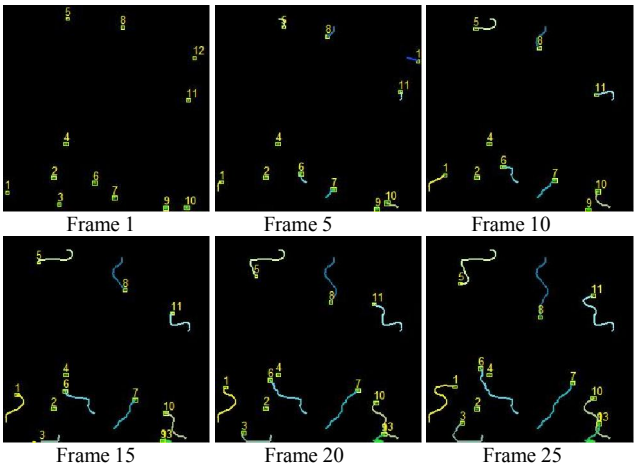

Fig. 4 Tracking results using ANT Estimator

As shown in Fig.3 and 4, our algorithm performs well, and it track successfully new entering cells and disappearing cells (i.e., cell 3, disappearing at frame 5, and re-entering at frame 15). Similarly, PF can achieve same results for this case.

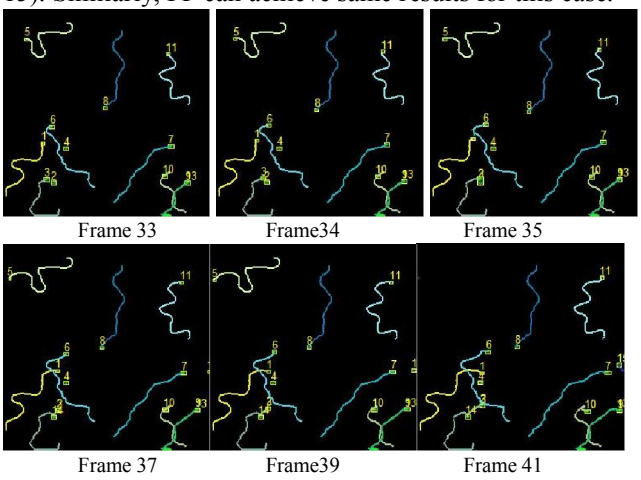

Fig. 5 Tracking results using PF

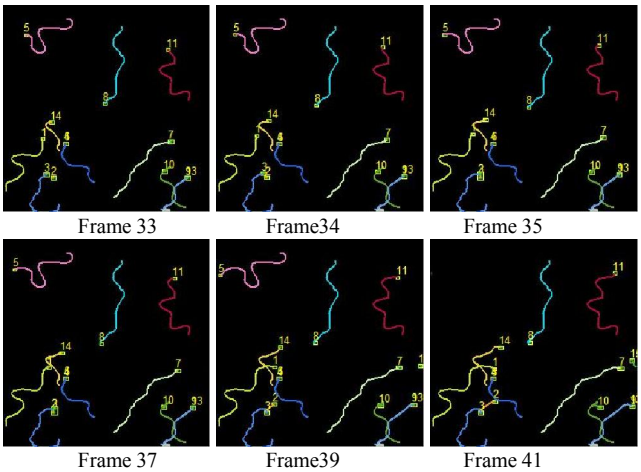

Fig. 6 Tracking results using ANT Estimator

Fig. 5 and 6 illustrate the results for close cells (cell 2 and 3) using the ANT Estimator and PF. It can be observed that the tracks of cells 2 and 3 are kept for ANT Estimator, while new cell track (i.e., cell 14) is initiated for PF.

Fig. 7 presents the run time comparison for each frame, and our proposed algorithm requires more computation burden due to probabilistic selection decision. However, our algorithm can achieve better accuracy in terms of the recorded number of cells in each frame, as shown in Fig. 8.

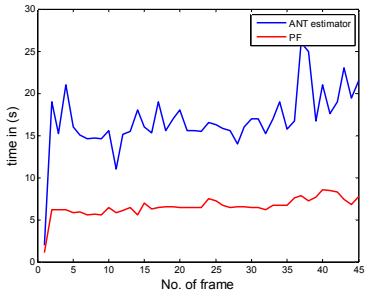

Fig. 7 Tracking time comparison for each frame

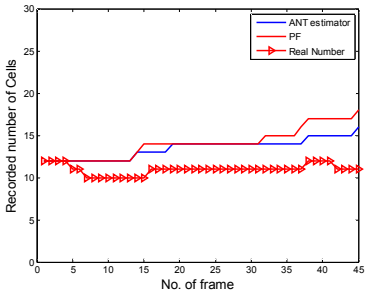

Fig. 8 Recorded tracking number comparison for each frame

V. Conclusion

In this paper, we develop a novel parameter estimate algorithm, which is based on ant stochastic searching behavior. Through modeling decision of each ant, we can make ants successfully track detected cells. Simulation results show that our algorithm can deal with cases such as entering or disappearing observation field, and occlusion. Further research is required to gain accurate dynamic parameter such as velocity and acceleration.

Acknowledgment

This work is supported by Natural Science Foundation of China（No. 61273312）, Natural Science Foundation of Jiangsu Province （No.BK2010261）, and Cooperation Innovation of Industry, Education and Academy of Jiangsu Province (No. BY2010126）.

References

[1] Erik M., Oleh D., Ihor S., Wiggert A. van Cappellen, “Tracking in cell and developmental biology”, Seminars in Cell & Developmental Biology, Vol. 20, no. 8, pp. 894-902, Oct, 2009.

[2] Stephens DJ, Allan VJ, “Light microscopy techniques for live cell imaging,” Science, Vol. 300, pp. 82 - 86,2003.

[3] Pawley JB. Handbook of biological confocal microscopy. 3rd ed. New York:Springer; 2006.

[4] Zhou, S.K., Chellappa, R., Moghaddam, B, “Visual tracking and recognition using appearance-adaptive models in particle filters,” IEEE Trans. Imaging Process. Vol. 13, pp. 1491 - 1506, 2004.

[5] B. N. Vo, S. Singh, and A. Doucet, "Sequential Monte Carlo methods for multi-target filtering with random finite sets," IEEE Trans.Aerospace & Electronic Systems, vol. 41, no. 4, pp. 1224–1245, Oct. 2005.

[6] B.-T. Vo, B.-N. Vo, and A. Cantoni, "Analytic implementations of the cardinalized probability hypothesis density filter," IEEE Trans.Signal Processing, vol. 55, no. 7, pp. 3553–3567, 2007.

[7] B.-N. Vo and W.-K. Ma, "The Gaussian mixture probability hypothesis density filter," IEEE Trans. Signal Processing, vol. 54, no. 11,pp. 4091–4104, Nov. 2006.

[8] B.-T. Vo, B.-N. Vo, and A. Cantoni, "The cardinality balanced multi-target multi-Bernoulli filter and its implementations," IEEE Trans. Signal Processing, Vol. 57, No. 2, pp. 409–423, Feb. 2009.

[9] K. Li, E. Miller, L. Weiss, P. Campbell, and T. Kanade, "Online tracking of migrating and proliferating cells imaged with phase-contrast microscopy," in *2006 Conf. Comput. Vision Pattern Recognit.Workshop (CVPRW'06)*, New York,, Jun. 2006, pp. 65–72.

[10] H. Shen, G. Nelson, S. Kennedy, D. Nelson, J. Johnson, D. Spiller, M.R. H. White, and D. B.Kell, "Automatic tracking of biological cells and compartments using particle filters and active contours," *Chem. Intell.Lab. Syst.*, vol. 82, no. 1–2, pp. 276–282, May, 2006.

[11] Ihor Smal, Katharina Draegestein, Niels Galjart, et al, "Particle Filtering for Multiple Object Tracking in Dynamic Fluorescence Microscopy Images: Application to Microtubule Growth Analysis," IEEE Trans. on Medical Imaging, Vol. 27, no. 6, pp.789-804 , June 2008

[12] J. Heinonen, F. Pettersson, Hybrid ant colony optimization and visibility studies applied to a job-shop scheduling problem, Applied Mathematics and Computation (2006), doi:10.1016/j. amc.2006.09.023.

[13] Benlian Xu, Huigang Xu, Jihong Zhu, "Ant Clustering PHD Filter for Multiple-Target Tracking. Applied Soft Computing," Vol. 11, no. 1, pp. 1074-1086, (2011.

[14] Benlian Xu, Jihong Zhu, Huigang Xu, "An ant stochastic decision based particle filter and its convergence," Signal Processing, Vol. 90, No. 9,pp. 2731-2748, 2010.